Front. Phys., 2014, 9(5): 587–597
DOI 10.1007/s11467-014-0421-5

REVIEW ARTICLE

Quantum information processing and metrology with color centers in diamonds

Jing-Wei Zhou, Peng-Fei Wang, Fa-Zhan Shi, Pu Huang, Xi Kong, Xiang-Kun Xu, Qi Zhang, Zi-Xiang Wang, Xing Rong, Jiang-Feng Du†

Hefei National Laboratory for Physics Sciences at the Microscale and Department of Modern Physics, University of Science and Technology of China, Hefei 230026, China

Corresponding author. E-mail: †*djf@ustc.edu.cn*

Received July 19, 2013; accepted March 3, 2014

The Nitrogen–Vacancy (NV) center is becoming a promising qubit for quantum information processing. The defect has a long coherence time at room temperature and it allows spin state initialized and read out by laser and manipulated by microwave pulses. It has been utilized as a ultra sensitive probe for magnetic fields and remote spins as well. Here, we review the recent progresses in experimental demonstrations based on NV centers. We first introduce our work on implementation of the Deutsch–Jozsa algorithm with a single electronic spin in diamond. Then the quantum nature of the bath around the center spin is revealed and continuous wave dynamical decoupling has been demonstrated. By applying dynamical decoupling, a multi-pass quantum metrology protocol is realized to enhance phase estimation. In the final, we demonstrated NV center can be regarded as a ultra-sensitive sensor spin to implement nuclear magnetic resonance (NMR) imaging at nanoscale.

Keywords quantum information processing and metrology, Nitrogen–Vacancy center, phase estimation, dynamical decoupling, single spin detection

PACS numbers 03.67.Mn, 04.70.Dy, 89.70.Kn

Contents

1 Introduction

For many years spins in solid states, such as quantum dots [1] and phosphorus defect in silicon [2], have drawn the attention of scientists in order to achieve quantum information processing. Most of these systems require cryogenic condition, as they strongly couple to vibrations, excitations or electron spin baths. In contrast, the defects in diamonds have shown the excellent isolated structure resulting the very long coherence time at room temperature, which makes it share the nice property of single atoms. The defect consists of a substitutional ^{14}N atom and a vacancy in an adjacent site. The centers are often created by ion implantation and annealed in bulk or nanocrystalline diamonds. In the Nitrogen–Vacancy (NV^-) center, six electrons occupy the dangling bonds of the vacancy complex forming the C_{3v} point symmetry. The ground and excited electron states are spin triplets ($S = 1$) with an optical transition between ^{3}A and ^{3}E with a zero-phonon line at 1.945 eV. With a home-built scanning confocal microscopy, the locations of individual NV centers can be addressed. Moreover, it can be polarized and read out by 532 nm green laser and coherently controlled by applying an resonant microwave

Frontiers of Physics

driving field.

NV centers are thought as a promising candidate for quantum information processing [3, 4] and quantum metrology [5]. Quantum logic gate [6, 7], quantum entanglement generation [8, 9], a long life quantum memory [10, 11] and single-shot read out has been realized in NV center system [12–14]. Quantum algorithms [15, 16] have been also demonstrated in such systems. Direct spin coupling [17] between NV centers and entanglement between a single NV center and photons [18] makes NV center an excellent processor to build a scalable quantum computer. Recently, by joint measurement of the photons, Hanson's group entangled two distant NV centers separated by 3 meters [19]. Combining the local long-lived nuclear spin registers [20, 21], the quantum network based on NV centers is promising. Experimental implementation of NV centers coupling to other qubits, such as superducting qubit [22, 23] are leading the way to hybrid quantum computation. The coupling to nanomechanical oscillator is also demonstrated [24, 25].

By employing its favorite coherence as well as its atomic-scale size, it has been used to image ultra-small signal such as magnetic and electric field with nanometer spatial resolution [26–29]. The NV center has also been realized as a sensitive nanoscale thermometer [30]. Moreover, as a pure quantum system, the center has been used to perform experiments to clarify fundamental issues such as Bell state violation [31] and "three-box" quantum game [32]. As a single photon source, the NV center has been utilized to demonstrate quantum cryptography [33] and the generation of single surface plasmons on silver nanowires [34].

We will introduce the structure and properties of the NV center and some experimental investigations in Section 2 to emphasize why the NV center is a good candidate in QIP. In Section 3, the Deutsch–Jozsa algorithm was demonstrated in the defects. Furthermore, an anomalous decoherence effect was observed in the NV centers and the quantum nature of the bath around the center spin is revealed in Section 4. In Section 5 we will show NV center as a ultra-sensitive sensor spin to implement NMR imaging at nanoscale.

2 NV centers

The NV center is one most common encountered color center in diamond. It consists of a vacancy in the vicinity of a nitrogen nuclear spin. Figure 1 shows the structure of an NV center in the diamond lattice and the energy level diagram. It has a spin-1 electron ground state. When a static magnetic field is aligned along the symmetry axis

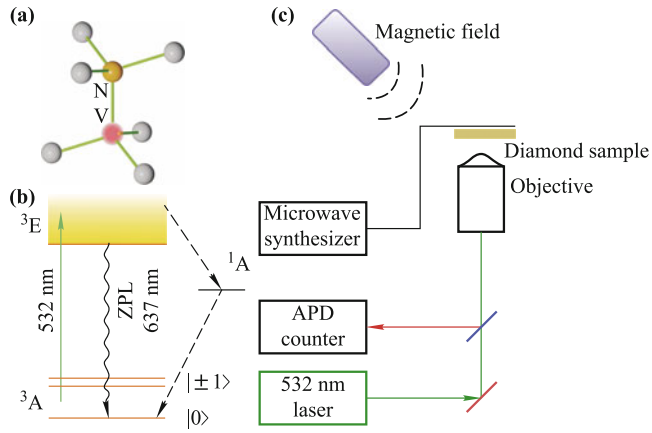

Fig. 1 **(a)** Atomic structure of an NV center in the diamond lattice. **(b)** Energy levels and optical transitions for optical pumping and detection of an NV center spin. **(c)** Schematic of the experiment setup.

([111] crystal axis) to degenerate the $m_s = \pm 1$ state, the system is described by the Hamiltonian:

$$H = DS_z^2 + g_e\mu_B B_z S_z + \sum_n \vec{S} \cdot \overleftrightarrow{A}_n \cdot \vec{I}_n \qquad (1)$$

Here D is the crystal field splitting which equals to 2.87 GHz and $\overleftrightarrow{A}_n$ is the coupling strength with the nearby ^{14}N nuclear (or ^{13}C). The hyperfine coupling between the NV center and the nearby nitrogen atom are about 2.2 MHz. To address different NV centers, a confocal microscopy system is used, which limits the optical lateral resolution of about 300 nm. With sub-diffraction imaging microscopy [35–37], a resolution of < 10 nm was achieved [38]. The laser pulse is controlled by an Acoustic–Optical Modulator (AOM). A single mode 532nm Nd:YAG frequency-doubled laser is applied to excite a single NV center via a high NA oil objective lens. A nano-position system is used to move the objective lens (or the diamond sample) to scan the diamond sample and locate the NV centers. The fluorescence photons come through a couple of 635nm–775nm filter, a pin-hole and finally arrive at the Avalanche Single-Photon Detector (APD) and turn into TTL signals. The TTL pulses are collected by a Data Acquisition board (DAQ). The fluorescence microscopy image of the single NV center will be recorded. A Hanbury–Brown–Twiss setup with two photo-detectors is used to measure the second order correlation function $g^2(\tau)$ to ensure a single NV is selected. One of the most attractive property is that the system can be cooled to the $m_s = 0$ by 532 nm laser at room temperature. This is due to the existence of the meta-stable state ^{1}A between the ground state and the excited state as shown in Refs. [39, 40]. Under the laser excitation, there are some probability for electron to decay from ^{3}E to ^{1}A which further decays

to $m_s = 0$ only, resulting the probability in $m_s = 0$ becomes larger. At room temperature, such process leads to initial state preparation of $|0\rangle$ state with fidelity larger than 90% [40]. For the ground state (denote as the center spin hereafter), an external magnetic field along [111] axis is used to lift the degeneracy between $|+1\rangle$ and $|-1\rangle$ and microwave pulses can be used to coherently excite the transition of $|0\rangle \leftrightarrow |1\rangle$ and $|0\rangle \leftrightarrow |-1\rangle$. When the microwave frequency is resonant with one of the transitions, the fluorescence intensity decreases. Different MW pulses are switched on and off by MW PIN switches and coupled together by wide band power dividers. To radiate high MW magnetic field on the NV center, a 20 micron diameter copper wire or a coplanar waveguide is soldered close to the diamond surface. All the components, including AOM, DAQ and PINs are synchronized and triggered by a pulse generator on a workstation.

As an open quantum system, such a ground state suffers coupling to the environment which leads to the loss of coherence. There are two kinds of the source contributing to the decoherence of the center spin: one is the N electron spin which is known as fast bath [41, 42], which can be removed by sample preparation [10]; the other is nuclear spin bath which is essentially non-Markova [43]. Such a bath arises from the existence of ^{13}C nuclear spin with a natural abundance of 1.1%. Theoretically, the decoherence behaviors can be described by the dipole interaction between the central spin and the bath as well as the dynamical of the bath [41, 43, 44]. This can be used to detect weak fields with nanoscale spatial resolution, which has significant applications in the biological and physical sciences [45, 46]. In this paper, we will briefly introduce the experimental progress in NV centers in our lab and exhibit the advantages of the defect as a candidate of quantum information processing and metrology.

3 Quantum algorithm

Since many basic QIP protocols has been demonstrated in NV centers, it is rather convincing that quantum computers based on diamond architecture are promising in future. Therefore, we report the first real quantum algorithm in NV centers, Deutsch–Jozsa (D–J) algorithm [45]. The D–J algorithm is a quantum algorithm proposed by Deutsch and Jozsa in 1992 [47]. In the D–J problem, a black box known as an oracle implements the function $f : \{0,1\}^n \to \{0,1\}$. The function is either constant (0 on all inputs or 1 on all inputs) or balanced (returns 1 for half of the input domain and 0 for the other half); the task is to determine whether f is constant or balanced by using the oracle. In the classical solution, $2^{n-1}+1$ evolutions of f will be required in the worst situation. The D–J quantum algorithm produces an answer that is always correct with a single evaluation of f. In general D–J algorithm, there are Hadamard gates and f-controlled gates to realize the algorithm. For single qubit, that is to say, the simplest situation in D–J algorithm, the initial state $|0\rangle$ is transferred to $\frac{|0\rangle+|1\rangle}{\sqrt{2}}$ as the input state with a Hadamard gate. Then the f-controlled gate follows. The f-controlled gate is defined as $V_f|z\rangle = (-1)^{f(z)}|z\rangle$, where z are 0, 1 and $f(z)$ is embodied by four functions with $f_1(z) = 0$, $f_2(z) = 1$ for constant function and $f_3(z) = z$, $f_4(z) = 1 - z$ for balanced function. So V_{fi} can be explicitly written by $V_{f1} = -V_{f2} = \begin{pmatrix} 1 & 0 \\ 0 & 1 \end{pmatrix}$; $V_{f3} = -V_{f4} = \begin{pmatrix} 1 & 0 \\ 0 & -1 \end{pmatrix}$. After the f-controlled gate, the input state evolves into $\frac{(-1)^{f_i(0)}|0\rangle+(-1)^{f_i(1)}|1\rangle}{\sqrt{2}}$ with $i = 1, 2, 3, 4$. Then through the other Hadamard gate, the output state would be detected by $|0\rangle$ or $|1\rangle$. Thus the two different functions can be distinguished by just single measurement of the

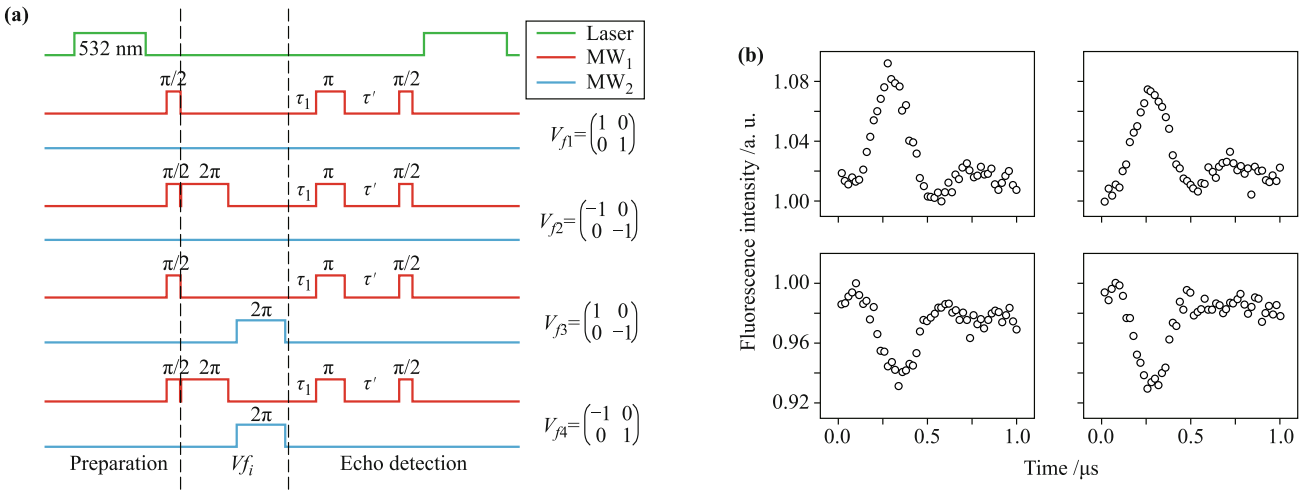

Fig. 2 **(a)** Diagram of the experimental pulse sequences used to realize the RDJ algorithm. **(b)** The output of the RDJ algorithm is detected by the spin echoes.

output state. In the experiment, we implement the D–J algorithm by encoding both a qubit and an auxiliary state in the $S = 1$ electron spin of an NV center. The Hadamard gates and the controlled f gate are realized with the microwave pulse sequences (see Fig. 2). First we exert a 20 Gauss magnetic field to split the energy level, so the microwaves would not affect each other. We use the $m_s = -1$ and $m_s = 0$ as the work qubit, and the $m_s = 1$ as an auxiliary state. In the Fig. 2, the 532 nm green laser pulse initialize the NV center to the $m_s = 0$ state. The $\pi/2$ pulse as the role of Hadamard gate makes a superposition state between $m_s = 0$ and $m_s = -1$. The different pulse sequences between the two black vertical line are to realize different controlled f gate V_{f1}, V_{f2}, V_{f3}, V_{f4}, then the following pulses sequence and the laser is used to read out the output results. In the experiment, the length of the π pulse is about 70 ns. Because the dephasing time ($T_2^* \approx 150$ ns) is too short to manipulate, we choose the Hahn echo ($T_2 \approx 2.9$ μs) to read out the experimental results. As the theoretical analysis, we expected a positive echo for the constant function and a negative echo for the balanced function. The experiment result in Fig. 2 is as expected. This is the first implementation of a quantum algorithm on individual spins at room temperature, indicating the NV center a promising candidate for quantum information processing. Another well-known quantum algorithm, Grover's search algorithm, is demonstrated in an electron-nuclear spin register [16]. These experiments demonstrate the power of quantum computation at room temperature in a real solid system, even though the large scale qubits are needed for practical quantum computing.

4 Decoherence

4.1 Anomalous decoherence effect

Decoherence is a key issue to modern quantum science and one of the main obstacles in processing large-scale quantum computation. The decay of electronic spin coherence due to interactions with surrounding nuclei has been a subject of a number of theoretical studies [48–51]. Such coupling is usually understood as classical noises, such as in the spectral diffusion theories, which are widely used in, e.g., magnetic resonance spectroscopy [52, 53] and optical spectroscopy [54, 55]. Decoherence occurs in a semiclassical environment whenever a qubit is subjected to a classical noise $\beta(t)$. The basic mechanism is described by a pure dephasing Hamiltonian

$$H = [\Omega + \beta(t)]S_z \tag{2}$$

Considering a coherent superposition state

$$|\phi\rangle = (|0\rangle + |1\rangle)/\sqrt{2} \tag{3}$$

Through a free evolution time τ, the two basis states will acquire a relative phase $\int \beta(t)\mathrm{d}t$ between them. After another $\pi/2$ pulse, the populations $p_0(t)$ of the $m_s = 0$ will be described as

$$p_0(t) = \frac{1}{2}(1 + \langle \exp[\mathrm{i} \int \beta(t)\mathrm{d}t]\rangle_\beta) \tag{4}$$

where $\langle \exp[\mathrm{i} \int \beta(t)\mathrm{d}t]\rangle_\beta$ denotes the average over all realizations of the random process. The ensemble average over all possible realizations of the random noise $\beta(t)$ gives the decay of the off-diagonal density matrix elements, i.e., the decoherence of the qubit.

Generally, it is believed stronger noises cause faster decoherence. However, Liu *et al.* recently found an opposite case according to the theoretical calculations [56]. Then, our group demonstrated the anomalous decoherence effect which was in a good agreement with the theoretical results [57].

We focus on the NV center in type IIa diamond, which coupled the nearby nuclear spin bath of nanometers size. Therefore, the environment itself is of quantum nature. Liu *et al.* compared the classical and quantum bath and predicted that the multi-transition can have longer coherence time than the single-transition under dynamical decoupling control, even though the former suffers stronger noises. In our experiment, a weak magnetic field (< 20 Guass) is applied along the NV axis to split $|+1\rangle$ and $|-1\rangle$. The triplet spin has both the single-transitions $|0\rangle \leftrightarrow |1\rangle$ and the double-transition $|+\rangle \leftrightarrow |-\rangle$. The single-transition coherence and the double-transition coherence are measured for a single NV center [see Fig. 3(a)]. In this sense, the double-transition is subjected to stronger noises and is expected to have shorter coherence time. These are confirmed by the FID, with the coherence time of the double-transition ($T_2^* = 1.82 \pm 0.08$ μs) and that of the single-transition ($T_2^* = 3.97 \pm 0.18$ μs). To further explore the quantum nature of the nuclear spin bath, we employ the multi-pulse dynamical decoupling control to elongate the center spin coherence time and to make the control effects on the quantum bath more pronounced. Amazingly, with increasing the number of control pulses, the double-transition coherence time increases more than that of the single-transition. Under the five-pulse control, the double-transition has significantly longer coherence time than the single-transition [Fig. 3(b)]. Such counterintuitive phenomena unambiguously demonstrate the quantum nature of the nuclear spin bath. Our observation of the ADE using NV center coherence establishes the quantum nature of nuclear spins bath at room temperature. Previous studies on coherence control of NV center spins in electron-spin baths

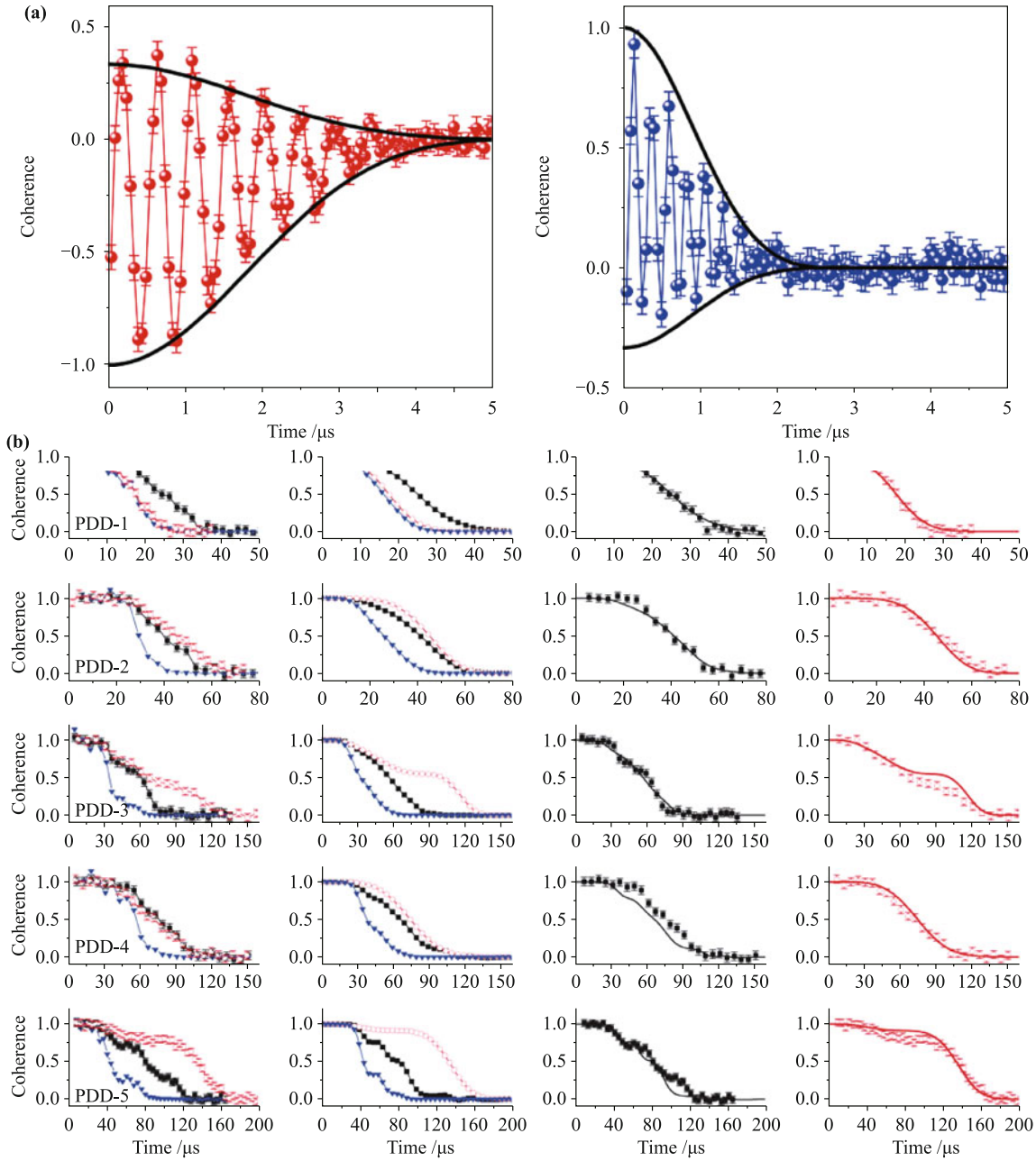

Fig. 3 **(a)** Measured and calculated free-induction decay of the single- and double-transition coherence. **(b)** Measured single- and double-transition coherence, under PDD-1 to PDD-5, from top to bottom.

[58] show that the decoherence there is well described by the classical noise theory. The fundamental difference between nuclear spin baths and electron-spin baths lies in the intra-bath interaction strength relative to the bath-center spin coupling. These works indicate that the ADE is insensitive to the details of the decoherence mechanisms, but is a universal phenomena due to the quantum nature of the bath.

4.2 Transitions from classic to quantum bath

To further understand the nature of the bath surrounding the center spin, we try to tune the ^{13}C nuclear bath into different regimes, classical bath or quantum bath [59]. Different with the semi-classical picture [52], the decoherence occurs where the system entangles with the surrounding nuclear spins [60]. The Hahn echo signal often shows a decay modulated by collapses and revivals at the Larmor frequency of the surrounding ^{13}C bath. Such collapses and revivals can be explained independently by decoherence [43] as well as classical dephasing [61]. The nuclear bath can be treated as a classical magnetic field noise with a spectral density peaked around the ^{13}C

Larmor frequency or the spin ensembles entangled with the center spin. To distinguish these two scenarios, we focus on the double-quantum transitions and the single-quantum transitions. The key idea is similar to ADE: the revivals would disappear in the case of quantum bath, but still exist when the classical spin noise dominates. We performed Hahn-echo spectroscopy on the single quantum transitions $|m_s = 0\rangle \rightarrow |m_s = -1\rangle$ and the double-quantum transition $|m_s = -1\rangle \rightarrow |m_s = +1\rangle$ in a static magnetic field varying between 40 and 140 G. The experimental results are presented in Fig. 4(a). On the double-quantum transition, coherence decays in few microseconds and never revives. However, for large fields, we observe a qualitatively different behavior: revivals appear also on the double-quantum transition, indicating that the carbon bath is tuned into a classical regime at high fields. We can dividing different shells according to the the strength of the electron–nuclear coupling $B_{\mathrm{NV},n}$ [see Fig. 4(b)]. The weakly coupled nuclei in outer shell ($B_{\mathrm{NV},n} \ll B$) can be treated as a classical noise field, for the long distance from the center spin. Quantum decoherence can only be caused by the inner shell of strongly coupled nuclei ($B_{\mathrm{NV},n} \gg B$).

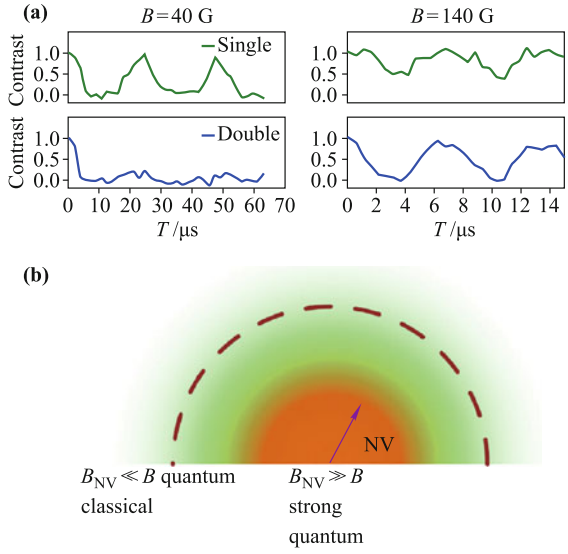

Fig. 4 **(a)** Hahn-echo measurements on the single quantum transitions and the double-quantum transition for varying magnetic fields. **(b)** Shells of the nuclear spin bath, defined by the strength of the NV magnetic field.

By adjusting the external magnetic field, we have demonstrated that the nuclear spin environment of NV centers can be tuned into two regimes: a strongly coupled quantum regime, where decoherence is due to back action of the NV center on the bath and a weakly coupled regime, where the bath is manifestation of a classical magnetic field noise.

4.3 Continues wave dynamical decoupling

In order to achieve reliable quantum-information processor, we would not only protect the coherence of the qubit but also implement the qubit manipulation [62]. However, the typical decoupling sequence actually freezes the qubit dynamics and hence conflicts with qubit manipulations. Using a continuous-wave dynamical decoupling (CWDD) method [24, 63, 64], both the gate operation and the coherence protection can be realized in the same time. The basic principle of CWDD can be understand as the system is transferred to a space spanned by dressed basis state, in which the noise is suppressed. This can be realized by applying two off-resonant continuous microwave driving fields $|0\rangle \rightarrow |\pm 1\rangle$ at the same time. The Hamiltonian of the NV center driven by two microwaves of the same off-resonance Δ and Rabi frequency Ω can be written in the interaction picture as follows:

$$H = DS_z^2 + \gamma_e B S_z + \sqrt{2}\Omega_1 \cos(\omega_1 t) S_x + \sqrt{2}\cos(\omega_2 t) S_x \tag{5}$$

where $\Delta = D + \gamma_e B - \omega_1 = D - \gamma_e B - \omega_1$. The diagonalization of H_{NV} results in three dressed states, $|e\rangle$, $|d\rangle$, $|g\rangle$ in the driven space. Owing to the symmetry of H_{NV} and nonzero Ω, the energies of all the three states are only functions of b^2, which are insensitive to b. Hence, the dephasing between $|d\rangle$ and $|g\rangle$ will be strongly suppressed when the microwave Rabi frequency Ω is much larger than the weak effective random field. With the appropriate ratio of $\Omega/\Delta = 4$, even the b^2 term in ω_{dg} is eliminated so that the lowest order is $\sim b^4$, and a much greater coherence time can be achieved in the protected subspace spanned by $|d\rangle$ and $|g\rangle$.

After the initialization of $|0\rangle$, two driven microwaves (MW1, MW2) are up-ramped linearly to prepare $|g\rangle$ adiabatically, the RF is used for the qubit manipulation encoded in the driven system with the continuous microwave protection, and finally the down-ramped microwaves map the encoded state to $|0\rangle$ for laser readout. The FID signal for the CWDD-protected subspace $|d\rangle, |g\rangle$ obtained by applying a detuned RF pulse is shown in Fig. 5(a), corresponding $T^*_{2,\mathrm{CWDD}} = 18.9$ μs. This shows that the coherence time of the CWDD-protected single spin is prolonged by ~ 20 times from the coherence time of the bare spin (about 0.93 μs) of the NV center. Moreover, by comparing the Rabi oscillation in bare basis and dressed basis [Fig. 5(b)], it is clear that the oscillations is well preserved in driven space almost without decay even after 25 μs.

Different with conventional dynamical decoupling [58, 65], the qubit gate and the coherence protection are both realized in CWDD. Another approach demonstrated by

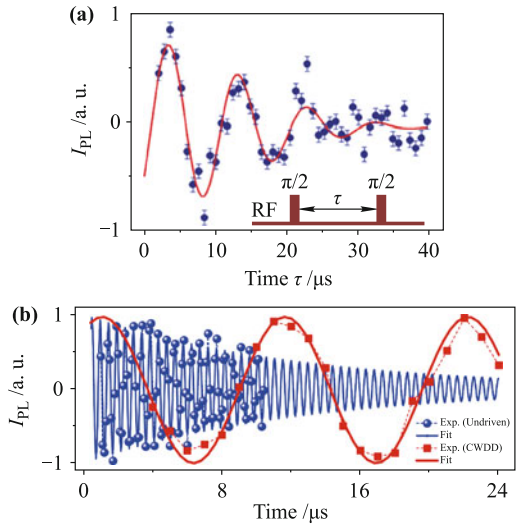

Fig. 5 **(a)** Experimental FID signals in the NV center driven system. **(b)** Measured decay of Rabi oscillation both in the undriven space and in the subspace protected by CWDD.

group from Delft University of Technology is to combine dynamical decoupling of the electron spin and continuous nuclear spin driving [16].

5 Quantum metrology

5.1 Phase estimation

Quantum metrology makes use of quantum coherence to reach higher sensitivity than the classical method known as standard quantum limit (SQL) [66–70]. Most previous studies are focusing on employing entanglement to realize sensitivity overcoming SQL. Though many impressive experiments have been carried out based on different system, the improvement is limited due to the small number of entangled qubits. On a paralleled way, An entanglement free Multi-Pass (MP) protocol is proposed to beat SQL, and very recently, a remarkable experiment is carried out on linear optical [71] and significant improvement is reached. However, the sensitivity is limited by the loss of coherence which plays the central role in MP. In our experiment, we used MP to improve the sensitivity of the phase estimations [72]. To do this, we employ the idea of Aharonov–Anandan geometric phase (AA phase) which maps an unknown phase difference of the microwave ϕ into the relative phase of two quantum state $|0\rangle$ and $|1\rangle$. By measuring this phase factor, we get the knowledge of ϕ with a precision of γ (the measurement efficiency). By repeating such process N times, the phase estimation precision scales as $\gamma/\sqrt{N}$. On the other hand, if the coherence of the two state is long enough, we can repeat such process N times and a phase factor $N\phi$ is accumulated, the corresponding estimation precision is γ/N. Given the same repetition times, the precision of the later scheme can beaten that of the previous one as $1/\sqrt{N}$. In our experiment, we first initialized the system to $|0\rangle$ by 532nm laser and then generated the coherence state $|0\rangle$ and $|+1\rangle$ by a $\pi/2$ pulse along the x axis. With the assistance of the third level $|-1\rangle$, we executed the geometrical path under two microwave π pulse to generate the AA phase, such a geometrical path is future repeated N times before read out. And then, we detected the accumulated AA phase with a second $\pi/2$ pulse followed by a standard Rabi Oscillation measurement along the y axis. As is shown above, the coherence is the key issue in our experiment, as the repetitions times increase, decoherence would corrupted the result [Fig. 6(a)]. However, the decoherence can be suppressed by DD pulse. In the experiment, we employed CPMG to prolong the coherence time and correspondingly, the phase estimation precisions further increase [Fig. 6(b)]. Under CPMG7, our method realize a precision enhancement factor of $\sim$ 24 when compared with the result based on one single geometric path and 4 folder when compared to its classical protocols with the same repetition times. Note that under CPMG5, the main limitation comes from the manipulation error rather than decoherence. In summary,

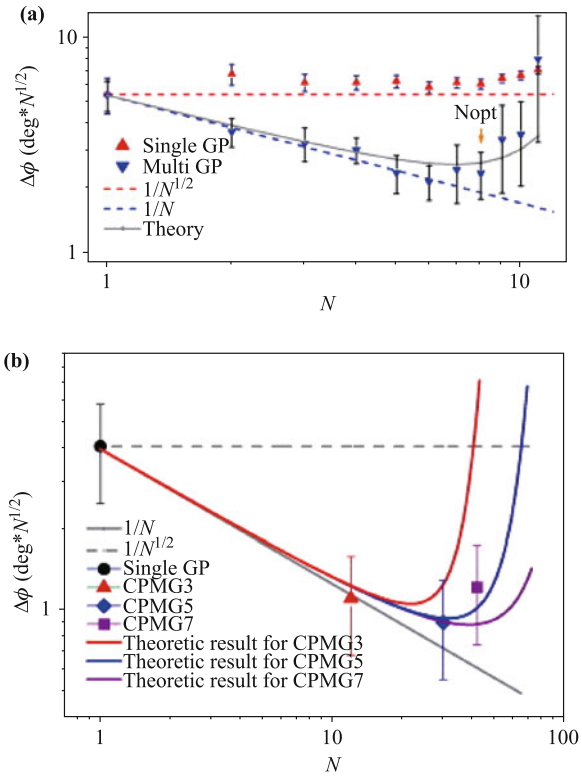

Fig. 6 **(a)** With N increases, $\Delta\phi$ ceases to scale with $1/N$ for the decoherence. **(b)** Results of multi-pass protocol under the protection of CPMG.

our experiment demonstrated the multi-pass quantum metrology protocol can be used to realize the higher sensitivity than the classical method, by employing DD, and the coherence time is prolonged and the sensitivity is improved. In the future, employing DD to entanglement-based quantum metrology is of interest.

5.2 Detection single electron and nuclear spins

NV center is also utilized as a spin sensor for detecting the surrounding single spins. Recently, We study an NV center, which was incidentally coupled to a single nearby spin with spin 1/2 [73]. This system can be modeled by a coupling Hamiltonian

$$H = DS_z^2 + \omega_s S_z + \omega_I I_z + S_z A I_z \tag{6}$$

To reveal the coupling, we use two protocols of spin-echo-detected double electron–electron resonance (known as SEDOR or DEER). In both schemes we address the effective two-level system of the NV spin S with a resonant microwave and perform a Hahn-echo measurement on this system. In this measurement, an initial $\pi/2$ pulse prepares the spin in a coherent superposition $|\psi(t=0)\rangle = (|0\rangle + e^{i\phi}|1\rangle)/\sqrt{2}$ with $\phi = 0$. ϕ evolves over time, is refocused by the π pulse at $t = \tau$ and converted into population by the final $\pi/2$ pulse. With replacing the π pulse on the dark spin by an ESR pulse sequence such as FID. In this way we measure the dark spin's coherence time $T_{2,e}^* = 2.3 \pm 0.1$ μs. The FID signal reveals a beating at 0.89 ± 0.03 MHz, which can be interpreted as a coupling of the dark spin to a nearby nuclear spin with $I = 1/2$. These measurements identify the dark spin as a nitrogen-related N2 defect by comparing the information we extracted about the hyperfine coupling and the g factor. Moreover, We polarize the NV and swap its state with the thermal state of the unpolarized dark spin and achieve a cooling efficiency of $p_0 = 14.3\%$. Recently, with cooperation with J. Wrachtrup's Group, we extended such sensing technique into nanoscale NMR [74]. The experimental setup is illustrated in Fig. 7(a), with a organic material sample on the diamond surface. The NV center was created near the surface < 10 nm. The technique for detecting the nuclear spin in the sample is based on measuring the spin noise near the NV center with a dynamical decoupling method. The nearby thermal nuclear spins will lead to a classical magnetic field noise with a spectral density peaked around the Larmor frequency. Using multi-pulse dynamical decoupling, spin noise from intrinsic nuclei of the diamond lattice is revealed in Fig. 7(b). Under high-order dynamical decoupling, the spectrum reveals an additional smaller peak [blue line in Fig. 7(b)]. The small peaks are attributed to protons from the sample placed on the diamond surface. Its frequency scales linearly with magnetic field [Fig. 7(b)] with a slope of 4.25 ± 0.04 kHz/G, the gyromagnetic ratio of ^{1}H. By comparing with a numerical simulation, the signal was generated by the 10^4 closest protons, corresponding to a detection volume of only $(5\ \text{nm})^3$. Such sensitivity is comparable to the state-of-art magnetic resonance force microscopy (MRFM), which allows detection and imaging of ensembles of nuclei in a virus particle [75]. In contrast to the ultralow temperatures needed in MRFM, diamond-based nanomagnetometer can image nulcear spins under ambient conditions. The single nuclear imaging in room temperature may be achieved in future with such a marvelous single center spin. Such nanoscale NMR would have significant impact on chemical and biological science.

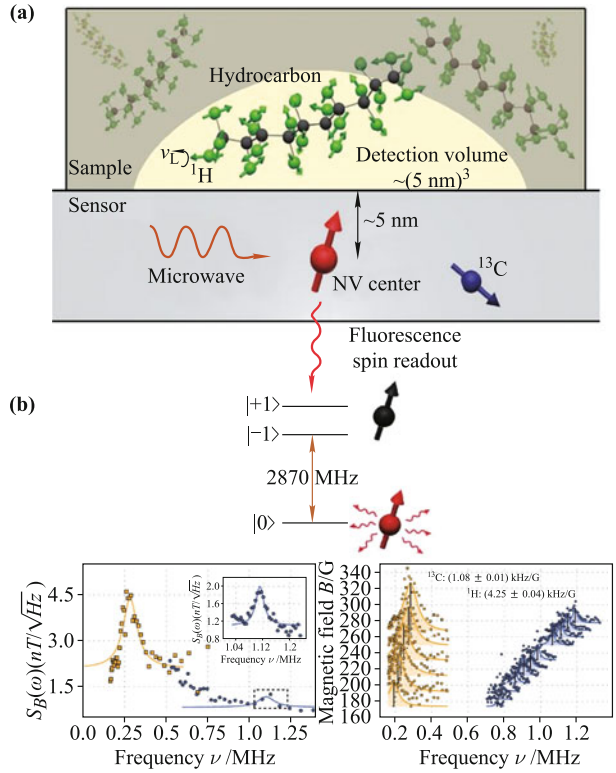

Fig. 7 **(a)** Experimental setup with the organic sample placed on the diamond surface. **(b)** NMR spectrum of nuclei around NV center.

6 Discussion and outlook

Ever since individual NV centers was controlled coherently, this atoms-like defect in diamonds has become a popular system favorable by many scientists. Applications such as magnetic sensing, single photon source are getting more and more efficient and practical. The advantage of high fidelity polarization and readout, easy

to rotation and long memory time in room temperature makes it a promising candidate to build quantum information processor. Also, there is plenty approaches proposed to make a large scale quantum computer based on diamonds. In the same time other defects are also drawing researchers' attention [3, 76]. By exploiting the center's property and the developing engineering technique, the road toward a room-temperature QIP device is promising.

Acknowledgements This work was supported by the National Key Basic Research Program of China (Grant No. 2013CB921800), the National Natural Science Foundation of China (Grant Nos. 11227901, 11275183, 91021005, and 10834005), the 'Strategic Priority Research Program (B)' of the CAS (Grant No. XDB01030400) and the Fundamental Research Funds for the Central Universities.

References

1. J. R. Petta, A. C. Johnson, J. M. Taylor, E. A. Laird, A. Yacoby, M. D. Lukin, C. M. Marcus, M. P. Hanson, and A. C. Gossard, Coherent manipulation of coupled electron spins in semiconductor quantum dots, *Science*, 2005, 309(5744): 2180
2. B. E. Kane, A silicon-based nuclear spin quantum computer, *Nature*, 1998, 393(6681): 133
3. J. Wrachtrup and F. Jelezko, Processing quantum information in diamond, *J. Phys.: Condens. Matter*, 2006, 18(21): S807
4. J. R. Weber, W. F. Koehl, J. B. Varley, A. Janotti, B. B. Buckley, C. G. Van de Walle, and D. D. Awschalom, Quantum computing with defects, *Proc. Natl. Acad. Sci. USA*, 2010, 107(19): 8513
5. V. Giovannetti, S. Lloyd, and L. Maccone, Quantum metrology, *Phys. Rev. Lett.*, 2006, 96(1): 010401
6. F. Jelezko, T. Gaebel, I. Popa, M. Domhan, A. Gruber, and J. Wrachtrup, Observation of coherent oscillation of a single nuclear spin and realization of a two-qubit conditional quantum gate, *Phys. Rev. Lett.*, 2004, 93(13): 130501
7. F. Jelezko, T. Gaebel, I. Popa, A. Gruber, and J. Wrachtrup, Observation of coherent oscillations in a single electron spin, *Phys. Rev. Lett.*, 2004, 92(7): 076401
8. P. Neumann, N. Mizuochi, F. Rempp, P. Hemmer, H. Watanabe, S. Yamasaki, V. Jacques, T. Gaebel, F. Jelezko, and J. Wrachtrup, Multipartite entanglement among single spins in diamond, *Science*, 2008, 320(5881): 1326
9. F. Dolde, I. Jakobi, B. Naydenov, N. Zhao, S. Pezzagna, C. Trautmann, J. Meijer, P. Neumann, F. Jelezko, and J. Wrachtrup, Room-temperature entanglement between single defect spins in diamond, *Nat. Phys.*, 2013, 9(3): 139
10. G. Balasubramanian, P. Neumann, D. Twitchen, M. Markham, R. Kolesov, N. Mizuochi, J. Isoya, J. Achard, J. Beck, J. Tissler, V. Jacques, P. R. Hemmer, F. Jelezko, and J. Wrachtrup, Ultralong spin coherence time in isotopically engineered diamond, *Nat. Mater.*, 2009, 8(5): 383
11. G. Fuchs, G. Burkard, P. Klimov, and D. Awschalom, A quantum memory intrinsic to single nitrogen–vacancy centres in diamond, *Nat. Phys.*, 2011, 7(10): 789
12. P. Neumann, J. Beck, M. Steiner, F. Rempp, H. Fedder, P. R. Hemmer, J. Wrachtrup, and F. Jelezko, Single-shot readout of a single nuclear spin, *Science*, 2010, 329(5991): 542
13. B. B. Buckley, G. D. Fuchs, L. C. Bassett, and D. D. Awschalom, Spin-light coherence for single-spin measurement and control in diamond, *Science*, 2010, 330(6008): 1212
14. L. Robledo, L. Childress, H. Bernien, B. Hensen, P. F. Alkemade, and R. Hanson, High-fidelity projective read-out of a solid-state spin quantum register, *Nature*, 2011, 477(7366): 574
15. F. Shi, X. Rong, N. Xu, Y. Wang, J. Wu, B. Chong, X. Peng, J. Kniepert, R. S. Schoenfeld, W. Harneit, M. Feng, and J. Du, Room-temperature implementation of the Deutsch–Jozsa algorithm with a single electronic spin in diamond, *Phys. Rev. Lett.*, 2010, 105(4): 040504
16. T. van der Sar, Z. H. Wang, M. S. Blok, H. Bernien, T. H. Taminiau, D. M. Toyli, D. A. Lidar, D. D. Awschalom, R. Hanson, and V. V. Dobrovitski, Decoherence-protected quantum gates for a hybrid solid-state spin register, *Nature*, 2012, 484(7392): 82
17. T. Gaebel, M. Domhan, I. Popa, C. Wittmann, P. Neumann, F. Jelezko, J. R. Rabeau, N. Stavrias, A. D. Greentree, S. Prawer, J. Meijer, J. Twamley, P. R. Hemmer, and J. Wrachtrup, Room-temperature coherent coupling of single spins in diamond, *Nat. Phys.*, 2006, 2(6): 408
18. E. Togan, Y. Chu, A. S. Trifonov, L. Jiang, J. Maze, L. Childress, M. V. G. Dutt, A. S. Sorensen, P. R. Hemmer, A. S. Zibrov, and M. D. Lukin, Quantum entanglement between an optical photon and a solid-state spin qubit, *Nature*, 2010, 466(7307): 730
19. H. Bernien, B. Hensen, W. Pfaff, G. Koolstra, M. S. Blok, L. Robledo, T. H. Taminiau, M. Markham, D. J. Twitchen, L. Childress, and R. Hanson, Heralded entanglement between solid-state qubits separated by three metres, *Nature*, 2013, 497(7447): 86
20. M. V. G. Dutt, L. Childress, L. Jiang, E. Togan, J. Maze, F. Jelezko, A. S. Zibrov, P. R. Hemmer, and M. D. Lukin, Quantum register based on individual electronic and nuclear spin qubits in diamond, *Science*, 2007, 316(5829): 1312
21. P. Neumann, R. Kolesov, B. Naydenov, J. Beck, F. Rempp, M. Steiner, V. Jacques, G. Balasubramanian, M. L. Markham, D. J. Twitchen, S. Pezzagna, J. Meijer, J. Twamley, F. Jelezko, and J. Wrachtrup, Quantum register based on coupled electron spins in a room-temperature solid, *Nat. Phys.*, 2010, 6(4): 249
22. X. Zhu, S. Saito, A. Kemp, K. Kakuyanagi, S. i. Karimoto, H. Nakano, W. J. Munro, Y. Tokura, M. S. Everitt, K. Nemoto, M. Kasu, N. Mizuochi, and K. Semba, Coherent

coupling of a superconducting flux qubit to an electron spin ensemble in diamond, *Nature*, 2011, 478(7368): 221

23. Y. Kubo, C. Grezes, A. Dewes, T. Umeda, J. Isoya, H. Sumiya, N. Morishita, H. Abe, S. Onoda, T. Ohshima, V. Jacques, A. Dréau, J.-F. Roch, I. Diniz, A. Auffeves, D. Vion, D. Esteve, and P. Bertet, Hybrid quantum circuit with a superconducting qubit coupled to a spin ensemble, *Phys. Rev. Lett.*, 2011, 107: 220501
24. P. Rabl, P. Cappellaro, M. V. G. Dutt, L. Jiang, J. R. Maze, and M. D. Lukin, Strong magnetic coupling between an electronic spin qubit and a mechanical resonator, *Phys. Rev. B*, 2009, 79(4): 041302
25. S. Kolkowitz, A. C. Bleszynski Jayich, Q. P. Unterreithmeier, S. D. Bennett, P. Rabl, J. G. E. Harris, and M. D. Lukin, Coherent sensing of a mechanical resonator with a single-spin qubit, *Science*, 2012, 335(6076): 1603
26. J. M. Taylor, P. Cappellaro, L. Childress, L. Jiang, D. Budker, P. R. Hemmer, A. Yacoby, R. Walsworth, and M. D. Lukin, High-sensitivity diamond magnetometer with nanoscale resolution, *Nat. Phys.*, 2008, 4(10): 810
27. G. Balasubramanian, I. Y. Chan, R. Kolesov, M. AlHmoud, J. Tisler, C. Shin, C. Kim, A. Wojcik, P. R. Hemmer, A. Krueger, T. Hanke, A. Leitenstorfer, R. Bratschitsch, F. Jelezko, and J. Wrachtrup, Nanoscale imaging magnetometry with diamond spins under ambient conditions, *Nature*, 2008, 455(7213): 648
28. J. R. Maze, P. L. Stanwix, J. S. Hodges, S. Hong, J. M. Taylor, P. Cappellaro, L. Jiang, M. V. G. Dutt, E. Togan, A. S. Zibrov, A. Yacoby, R. L. Walsworth, and M. D. Lukin, Nanoscale magnetic sensing with an individual electronic spin in diamond, *Nature*, 2008, 455(7213): 644
29. F. Dolde, H. Fedder, M. W. Doherty, T. Nobauer, F. Rempp, G. Balasubramanian, T. Wolf, F. Reinhard, L. C. L. Hollenberg, F. Jelezko, and J. Wrachtrup, Electric-field sensing using single diamond spins, *Nat. Phys.*, 2011, 7(6): 459
30. D. M. Toyli, C. F. de las Casas, D. J. Christle, V. V. Dobrovitski, and D. D. Awschalom, Fluorescence thermometry enhanced by the quantum coherence of single spins in diamond, *Proc. Natl. Acad. Sci. USA*, 2013, 110(21): 8417
31. G. Waldherr, P. Neumann, S. F. Huelga, F. Jelezko, and J. Wrachtrup, Violation of a temporal bell inequality for single spins in a diamond defect center, *Phys. Rev. Lett.*, 2011, 107(9): 090401
32. R. E. George, L. M. Robledo, O. J. E. Maroney, M. S. Blok, H. Bernien, M. L. Markham, D. J. Twitchen, J. J. L. Morton, G. A. D. Briggs, and R. Hanson, Opening up three quantum boxes causes classically undetectable wavefunction collapse, *Proc. Natl. Acad. Sci. USA*, 2013, 110(10): 3777
33. A. Beveratos, R. Brouri, T. Gacoin, A. Villing, J. P. Poizat, and P. Grangier, Single photon quantum cryptography, *Phys. Rev. Lett.*, 2002, 89(18): 187901
34. R. Kolesov, B. Grotz, G. Balasubramanian, R. J. Stohr, A. A. L. Nicolet, P. R. Hemmer, F. Jelezko, and J. Wrachtrup, Wave–particle duality of single surface plasmon polaritons, *Nat. Phys.*, 2009, 5(7): 470
35. S. W. Hell, Far-field optical nanoscopy, *Science*, 2007, 316(5828): 1153
36. S. W. Hell and M. Kroug, Ground-state-depletion fluorscence microscopy: A concept for breaking the diffraction resolution limit, *Appl. Phys. B*, 1995, 60(5): 495
37. P. Maurer, J. Maze, P. Stanwix, L. Jiang, A. Gorshkov, A. A. Zibrov, B. Harke, J. Hodges, A. S. Zibrov, A. Yacoby, D. Twitchen, S. W. Hell, R. L. Walsworth, and M. D. Lukin, Far-field optical imaging and manipulation of individual spins with nanoscale resolution, *Nat. Phys.*, 2010, 6(11): 912
38. E. Rittweger, K. Y. Han, S. E. Irvine, C. Eggeling, and S. W. Hell, STED microscopy reveals crystal colour centres with nanometric resolution, *Nat. Photonics*, 2009, 3(3): 144
39. J. Harrison, M. J. Sellars, and N. B. Manson, Optical spin polarisation of the N-V centre in diamond, *J. Lumin.*, 2004, 107(1–4): 245
40. N. B. Manson, J. P. Harrison, and M. J. Sellars, Nitrogen-vacancy center in diamond: Model of the electronic structure and associated dynamics, *Phys. Rev. B*, 2006, 74: 104303
41. R. Hanson, O. Gywat, and D. D. Awschalom, Room-temperature manipulation and decoherence of a single spin in diamond, *Phys. Rev. B*, 2006, 74(16): 161203
42. R. Hanson, V. V. Dobrovitski, A. E. Feiguin, O. Gywat, and D. D. Awschalom, Coherent dynamics of a single spin interacting with an adjustable spin bath, *Science*, 2008, 320(5874): 352
43. L. Childress, M. V. Gurudev Dutt, J. M. Taylor, A. S. Zibrov, F. Jelezko, J. Wrachtrup, P. R. Hemmer, and M. D. Lukin, Coherent dynamics of coupled electron and nuclear spin qubits in diamond, *Science*, 2006, 314(5797): 281
44. G. de Lange, T. van der Sar, M. S. Blok, Z. H. Wang, V. V. Dobrovitski, and R. Hanson, Controlling the quantum dynamics of a mesoscopic spin bath in diamond, arXiv: 1104.4648v1, 2011
45. F. Neugart, A. Zappe, F. Jelezko, C. Tietz, J. P. Boudou, A. Krueger, and J. Wrachtrup, Dynamics of diamond nanoparticles in solution and cells, *Nano Lett.*, 2007, 7(12): 3588
46. C. C. Fu, H. Y. Lee, K. Chen, T. S. Lim, H. Y. Wu, P. K. Lin, P. K. Wei, P. H. Tsao, H. C. Chang, and W. Fann, Characterization and application of single fluorescent nanodiamonds as cellular biomarkers., *Proc. Natl. Acad. Sci. USA*, 2007, 104(3): 727
47. D. Deutsch and R. Jozsa, Rapid solution of problems by quantum computation, *Proc. R. Soc. Lond. A*, 1992, 439(1907): 553
48. R. de Sousa and S. Das Sarma, Theory of nuclear induced spectral diffusion: Spin decoherence of phosphorus donors in Si and GaAs quantum dots, *Phys. Rev. B*, 2003, 68: 115322
49. W. M. Witzel, R. de Sousa, and S. Das Sarma, Quantum theory of spectral diffusion induced electron spin decoherence, *Phys. Rev. B*, 2005, 72: 161306(R)

50. W. Yao, R.B. Liu, and L. J. Sham, Theory of electron spin decoherence by interacting nuclear spins in a quantum dot, *Phys. Rev. B*, 2006, 74 (19): 195301
51. S. K. Saikin, W. Yao, and L. J. Sham, Single-electron spin decoherence by nuclear spin bath: Linked-cluster expansion approach, *Phys. Rev. B*, 2007, 75: 125314
52. P. W. Anderson, A mathematical model for the narrowing of spectral lines by exchange or motion, *J. Phys. Soc. Jpn.*, 1954, 9(3): 316
53. R. Kubo, Note on the stochastic theory of resonance absorption, *J. Phys. Soc. Jpn.*, 1954, 9(6): 935
54. P. R. Berman and R. G. Brewer, Modified optical Bloch equations for solids, *Phys. Rev. A*, 1985, 32(5): 2784
55. R. F. Loring and S. Mukamel, Unified theory of photon echoes: The passage from inhomogeneous to homogeneous line broadening, *Chem. Phys. Lett.*, 1985, 114(4): 426
56. N. Zhao, Z. Y. Wang, and R. B. Liu, Anomalous decoherence effect in a quantum bath, *Phys. Rev. Lett.*, 2011, 106 (21): 217205
57. P. Huang, X. Kong, N. Zhao, F. Z. Shi, P. F. Wang, X. Rong, R. B. Liu, and J. F. Du, Observation of an anomalous decoherence effect in a quantum bath at room temperature, *Nature Communications*, 2011, 2: 570
58. G. de Lange, Z. H. Wang, D. Riste, V. V. Dobrovitski, and R. Hanson, Universal dynamical decoupling of a single solid-state spin from a spin bath, *Science*, 2010, 330 (6000): 60
59. F. Reinhard, F. Z. Shi, N. Zhao, F. Rempp, B. Naydenov, J. Meijer, L. T. Hall, L. Hollenberg, J. F. Du, R. B. Liu, and J. Wrachtrup, Tuning a spin bath through the quantum-classical transition, *Phys. Rev. Lett.*, 2012, 108(20): 200402
60. W. H. Zurek, Pointer basis of quantum apparatus: Into what mixture does the wave packet collapse? *Phys. Rev. D*, 1981, 24(6): 1516
61. H. Bluhm, S. Foletti, I. Neder, M. Rudner, D. Mahalu, V. Umansky, and A. Yacoby, Dephasing time of GaAs electron-spin qubits coupled to a nuclear bath exceeding 200 μs, *Nat. Phys.*, 2011, 7(2): 109
62. X. K. Xu, Z. X. Wang, C. K. Duan, P. Huang, P. F. Wang, Y. Wang, N. Y. Xu, X. Kong, F. Z. Shi, X. Rong, and J. F. Du, Coherence-protected quantum gate by continuous dynamical decoupling in diamond, *Phys. Rev. Lett.*, 2012, 109: 070502
63. N. Timoney, I. Baumgart, M. Johanning, A. F. Varon, M. B. Plenio, A. Retzker, and C. Wunderlich, Quantum gates and memory using microwave-dressed states, *Nature*, 2011, 476(7359): 185
64. J. M. Cai, B. Naydenov, R. Pfeiffer, L. P. McGuinness, K. D. Jahnke, F. Jelezko, M. B. Plenio, and A. Retzker, Robust dynamical decoupling with concatenated continuous driving, *New J. Phys.*, 2012, 14(11): 113023
65. J. Du, X. Rong, N. Zhao, Y. Wang, J. Yang, and R. B. Liu, Preserving electron spin coherence in solids by optimal dynamical decoupling, *Nature*, 2009, 461(7268): 1265
66. J. A. Jones, S. D. Karlen, J. Fitzsimons, A. Ardavan, S. C. Benjamin, G. A. D. Briggs, and J. J. L. Morton, Magnetic field sensing beyond the standard quantum limit using 10-spin NOON states, *Science*, 2009, 324(5931): 1166
67. D. Leibfried, E. Knill, S. Seidelin, J. Britton, R. B. Blakestad, J. Chiaverini, D. B. Hume, W. M. Itano, J. D. Jost, C. Langer, R. Ozeri, R. Reichle, and D. J. Wineland, Creation of a six-atom 'Schrödinger cat' state, *Nature*, 2005, 438(7068): 639
68. T. Nagata, R. Okamoto, J. L. O'Brien, K. Sasaki, and S. Takeuchi, Beating the standard quantum limit with four-entangled photons, *Science*, 2007, 316(5825): 726
69. C. Gross, T. Zibold, E. Nicklas, J. Estve, and M. K. Oberthaler, Nonlinear atom interferometer surpasses classical precision limit, *Nature*, 2010, 464(7292): 1165
70. G. Y. Xiang, B. L. Higgins, D. W. Berry, H. M. Wiseman, and G. J. Pryde, Entanglement-enhanced measurement of a completely unknown optical phase, *Nat. Photonics*, 2011, 5(1): 43
71. B. L. Higgins, D. W. Berry, S. D. Bartlett, H. M. Wiseman, and G. J. Pryde, Entanglement-free Heisenberg-limited phase estimation, *Nature*, 2007, 450(7168): 393
72. X. Rong, P. Huang, X. Kong, X. Xu, F. Shi, Y. Wang, and J. Du, Enhanced phase estimation by implementing dynamical decoupling in a multi-pass quantum metrology protocol, *Europhys. Lett.*, 2011, 95(6): 60005
73. F. Z. Shi, Q. Zhang, B. Naydenov, F. Jelezko, J. F. Du, F. Reinhard, and J. Wrachtrup, Quantum logic readout and cooling of a single dark electron spin, *Phys. Rev. B*, 2013, 87: 195414
74. T. Staudacher, F. Shi, S. Pezzagna, J. Meijer, J. Du, C. A. Meriles, F. Reinhard, and J. Wrachtrup, Nuclear magnetic resonance spectroscopy on a (5-nanometer) 3 sample volume, *Science*, 2013, 339(6119): 561
75. C. Degen, M. Poggio, H. Mamin, C. Rettner, and D. Rugar, Nanoscale magnetic resonance imaging, *Proc. Natl. Acad. Sci. USA*, 2009, 106(5): 1313
76. W. F. Koehl, B. B. Buckley, F. J. Heremans, G. Calusine, and D. D. Awschalom, Room temperature coherent control of defect spin qubits in silicon carbide, *Nature*, 2011, 479(7371): 84